AFRL-RX-WP-JA-2015-0137

NOVEL AUTOMATIC ELECTROCHEMICAL-MECHANICAL POLISHING (ECMP) OF METALS FOR SCANNING ELECTRON MICROSCOPY (POSTPRINT)

J. Tiley and C.A. Crouse
AFRL/RXCM

K. Shiveley II and G.B. Viswanathan
UES, Inc.

A. Shiveley
Universal Technology Corporation

APRIL 2014
Interim Report

AIR FORCE RESEARCH LABORATORY
MATERIALS AND MANUFACTURING DIRECTORATE
WRIGHT-PATTERSON AIR FORCE BASE OH 45433-7750
AIR FORCE MATERIEL COMMAND
UNITED STATES AIR FORCE

NOTICE AND SIGNATURE PAGE

AFRL-RX-WP-JA-2015-0137 HAS BEEN REVIEWED AND IS APPROVED FOR PUBLICATION IN ACCORDANCE WITH ASSIGNED DISTRIBUTION STATEMENT.

//Signature//

MICHEAL E. BURBA, Project Engineer
Metals Branch
Structural Materials Division

//Signature//

DANIEL J. EVANS, Chief
Metals Branch
Structural Materials Division

//Signature//

ROBERT T. MARSHALL, Deputy Chief
Structural Materials Division
Materials And Manufacturing Directorate

REPORT DOCUMENTATION PAGE

Form Approved
OMB No. 0704-0188

1. REPORT DATE ***(DD-MM-YY)***
April 2014

2. REPORT TYPE
Interim

3. DATES COVERED ***(From - To)***
19 March 2014 – 31 March 2014

4. TITLE AND SUBTITLE
NOVEL AUTOMATIC ELECTROCHEMICAL-MECHANICAL POLISHING (ECMP) OF METALS FOR SCANNING ELECTRON MICROSCOPY (POSTPRINT)

5a. CONTRACT NUMBER
In-house

5b. GRANT NUMBER

5c. PROGRAM ELEMENT NUMBER
62102F

6. AUTHOR(S)
See back.

5d. PROJECT NUMBER
4349

5e. TASK NUMBER

5f. WORK UNIT NUMBER
X0W6

7. PERFORMING ORGANIZATION NAME(S) AND ADDRESS(ES)
See back.

8. PERFORMING ORGANIZATION REPORT NUMBER

9. SPONSORING/MONITORING AGENCY NAME(S) AND ADDRESS(ES)

Air Force Research Laboratory
Materials and Manufacturing Directorate
Wright-Patterson Air Force Base, OH 45433-7750
Air Force Materiel Command
United States Air Force

10. SPONSORING/MONITORING AGENCY ACRONYM(S)
AFRL/RXCM

11. SPONSORING/MONITORING AGENCY REPORT NUMBER(S)
AFRL-RX-WP-JA-2015-0137

12. DISTRIBUTION/AVAILABILITY STATEMENT
Distribution Statement A. Approved for public release; distribution unlimited.

13. SUPPLEMENTARY NOTES
Journal article published in *Micron 41*(2010) 615-621. ©2010 Elsevier Ltd. The U.S. Government is joint author of the work and has the right to use, modify, reproduce, release, perform, display or disclose the work. This report contains color. The final publication is available at http://dx.doi.org/10.1016/j.micron.2010.03.008

14. ABSTRACT

A low-stress automated polishing device was developed for preparing titanium and nickel alloys for scanning electron microscopy imaging. The system used pulsed electrochemical reactions within an alkaline electrolyte to generate a thin passivation layer on the surface of the sample, which was removed by the mechanical vibration of the system. The passivation layer development and removal were documented for Ti-6Al-4V and IN718 samples subjected to varying electrical potential cycles and polishing times. Results indicated that the applied cyclic potentials removed material faster than typical removal techniques. In addition, electron back scatter diffraction data showed a decrease in subsurface damage using the developed electrochemical-mechanical process compared to standard mechanical polishing techniques.

15. SUBJECT TERMS
titanium polishing, electron microscopy imaging, EBSD, electro-mechanical polishing

16. SECURITY CLASSIFICATION OF:			**17. LIMITATION OF ABSTRACT:**	**18. NUMBER OF PAGES**	**19a. NAME OF RESPONSIBLE PERSON** (Monitor)
a. REPORT	**b. ABSTRACT**	**c. THIS PAGE**			Micheal E. Burba
Unclassified	Unclassified	Unclassified	SAR	11	**19b. TELEPHONE NUMBER** *(Include Area Code)* (937) 255-9795

Standard Form 298 (Rev. 8-98)
Prescribed by ANSI Std. Z39-18

REPORT DOCUMENTATION PAGE

Form Approved
OMB No. 0704-0188

REPORT DOCUMENTATION PAGE Cont'd

6. AUTHOR(S)

J. Tiley and C.A. Crouse - AFRL/RXCM

K. Shiveley II and G.B. Viswanathan - UES, Inc.

A. Shiveley - Universal Technology Corporation

7. PERFORMING ORGANIZATION NAME(S) AND ADDRESS(ES)

AFRL/RXCM
2941 Hobson Way
Bldg 654, Rm 136
Wright-Patterson AFB, OH 45433

UES, Inc.
4401 Dayton-Xenia Rd.
Dayton, OH 45432-1894

Universal Technology Corporation
Wright-Patterson AFB, OH 45433

Micron 41 (2010) 615–621

Contents lists available at ScienceDirect

Micron

journal homepage: www.elsevier.com/locate/micron

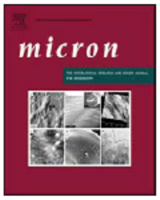

Novel automatic electrochemical–mechanical polishing (ECMP) of metals for scanning electron microscopy

J. Tiley[a,*], K. Shiveley II[b], G.B. Viswanathan[b], C.A. Crouse[a], A. Shiveley[c]

[a] *Air Force Research Laboratory, Materials and Manufacturing, Wright-Patterson AFB, OH 45433, United States*
[b] *UES Inc., Wright-Patterson AFB, OH 45433, United States*
[c] *Universal Technology Corporation, Wright-Patterson AFB, OH 45433, United States*

ARTICLE INFO

Article history:
Received 25 November 2009
Received in revised form 23 March 2010
Accepted 23 March 2010

Keywords:
Titanium polishing
Electron microscopy imaging
EBSD
Electro-mechanical polishing

ABSTRACT

A low-stress automated polishing device was developed for preparing titanium and nickel alloys for scanning electron microscopy imaging. The system used pulsed electrochemical reactions within an alkaline electrolyte to generate a thin passivation layer on the surface of the sample, which was removed by the mechanical vibration of the system. The passivation layer development and removal were documented for Ti–6Al–4V and IN718 samples subjected to varying electrical potential cycles and polishing times. Results indicated that the applied cyclic potentials removed material faster than typical removal techniques. In addition, electron back scatter diffraction data showed a decrease in subsurface damage using the developed electrochemical–mechanical process compared to standard mechanical polishing techniques.

Published by Elsevier Ltd.

1. Introduction

With growing use of advanced scanning electron microscopes (SEM) and the evaluation of hybrid and novel material systems, surface preparation of samples is an increasingly vital component in characterization of materials. State-of-the-art in surface preparation for titanium and Ni-base superalloys usually involves mechanical polishing from a diamond saw cut surface to a 6–3 μm finish. Samples for SEM characterization are typically final polished using 0.05 μm colloidal silica in a mechanical vibrating system (Vibromet^{TM}) (Tiley et al., 2004, 2009; Collins et al., 2009). Damage to the surface or subsurface of the material can adversely impact data quality captured by traditional backscatter electron imaging and electron backscatter diffraction (EBSD) techniques. Both techniques are widely used to characterize and incorporate microstructures of high strength titanium alloys and nickel-base superalloys into physics-based mechanical behavior models (Bieler et al., 2005; Salem and Semiatin, 2009; Meisenkothen et al., 2009). In addition, surface preparation techniques have a major impact on imaging ceramics and hybrid materials with ceramic components. Traditional mechanical sample preparation often liberates small precipitates and inclusions that damage the surface of the matrix materials and other phases within the hybrid material. The resultant microscratches are often difficult to remove from the surface and can cause significant subsurface damage, resulting in poor EBSD imaging.

The use of electrochemical techniques to form protective coatings on metallic surfaces has been well documented (Fontana, 1986; Jones, 1996; Reidenbach, 1994; Korb, 1994; Reed, 2006; Luetering et al., 2003). For example, applying a negative potential to metallic surfaces submerged in electrolyte removes metallic ions from the surface by electropolishing, which is used to prepare surfaces for scanning electron microscopy and various manufacturing processes. Although the process is used to prepare mechanical samples for EBSD measurements, the technique can produce surfaces with uneven polishing due to differences in the electrochemical reaction of phases and features within the sample. This process also can produce rounded edges on features above the surface of the sample where electrochemical response differs across an interface of the sample. The flatness of the sample surface is a major concern for characterizing γ' precipitates in nickel-base superalloys (Tiley et al., 2010; Kissinger, 1996).

On the other hand, applying positive potential to metal surfaces submerged in electrolyte forms an oxide layer on the metallic surface in a process known as anodization (Reidenbach, 1994; Korb, 1994). The anodic layer that forms on these materials had been characterized by many researchers and proven to provide significant corrosion resistance (Reed, 2006; Luetering et al., 2003). In titanium alloys, the pH of the electrolyte and the applied potentials controls the formation of the stable TiO_2 surface oxide layers. In particular, researchers found TiO_2 was stable in pH values between 8 and 10 for room temperature potentials between −0.1 V and 0.1 V

---

[*] Corresponding author at: Air Force Research Laboratory, AFRL/RXLM, 2230 Tenth Street, Building 655, Wright Patterson AFB, OH 45433, United States.
Tel.: +1 937 255 3514; fax: +1 937 255 3007.
E-mail address: jaimie.tiley@wpafb.af.mil (J. Tiley).

0968-4328/$ – see front matter. Published by Elsevier Ltd.
doi:10.1016/j.micron.2010.03.008

(Korb, 1994) in titanium–water systems. Multilayered scale with both Al_2O_3 and TiO_2 was found to form on Ti–6Al–4V samples that were oxidized in air at higher temperatures in a variety of environments (Du et al., 1996). Hydroxide films also formed when the potential was reduced below −1.2 for pH values between 7 and 10 (Korb, 1994). For nickel-base alloys, stable growth of Al_2O_3 and NiO oxide layers was documented under varying potential and pH conditions (Reidenbach, 1994; Boinet et al., 2003; Montemor et al., 2000). Mechanical polishing can be used to remove the anodic layer that adheres to the base material. The kinetics of the protective layer may be controlled using an applied voltage because the anodic layer is influenced by the electrochemical properties of the environment including the electrolyte bath. This provides a mechanism for controlling the formation of the passive films, which is called chemical–mechanical polishing.

Chemical–mechanical polishing (CMP) has been applied to fabricate micro-electro-mechanical systems where wafer planarization is an important component (Sniegowski, 1996). The alkaline chemistry of the slurry is thought to hydrolyze the oxide surface and weaken the bonding. The mechanical polishing removes the weakened oxide layers and provides faster removal of features that rise higher above the wafer surface. In CMP of titanium, the interaction of the sample surface with copper ions within the slurry increased the overall removal rate of the titanium by oxidizing the titanium metal and forcing the titanium into the slurry. The copper deposited onto the surface was removed by mechanical polishing faster than the titanium (Steigerwald et al., 1995). Consequently, the interactions of the material surface and slurry played a crucial rule in strengthening or weakening the bonding energy of the oxide layers.

Although the application of voltage during mechanical polishing has been previously suggested (Lee et al., 2006; Bonifas et al., 2004; Vander Voort, 2004) the use of a potential to create a protective film containing the surface damage for subsequent removal has not been well established. The proposed CMP process is expected to have a faster removal rate than either of the techniques alone. It is also expected to produce a superior surface for SEM characterization by reducing subsurface damage, precipitate pull-outs, and surface rounding common in mechanical polishing.

The subsurface damage and overall image quality of samples are difficult to assess quantitatively. However, qualitative assessment can be achieved by investigating the impact of subsurface damage on electron backscatter diffraction patterns (EBSD). Particularly, samples with higher subsurface damage produce poor EBSD patterns that are used to determine image quality (IQ). When these patterns are quantified by TSL^{TM} OIM Analysis [TexSEM, 2008], they produce low image quality (IQ) values. The software calculates the IQ values by summing the detected diffraction peaks in a given Hough Transform (TexSEM, 2001) which are influenced by retained surface damage and lattice strains accumulated from surface preparation.

The objective of this research effort is to develop and test an electro-chemical–mechanical sample preparation technique (ECMP) for titanium alloys (Ti–6Al–4V) and Ni-base superalloys (IN718). The technical goal is to limit the subsurface damage within the passivation film layer which is subsequently removed by mechanical and electro-chemical polishing.

2. Methods and procedures

2.1. Material used

Round bar Ti–6Al–4V test samples (0.5 in. surface diameter) with a colony microstructure were tested in the ECMP system. In addition, IN718 samples with a 0.5 in. × 0.25 in. rectangular surface area were used in the ECMP system. Thin sheet Ti–6Al–4V (0.025 in. thick) and IN200 (0.010 in. thick) were used for potential dynamic testing. The IN200 sheet material was used to provide the potential dynamic polarization curves based on availability of material. Because the chemistries of IN200 and IN718 are different, the data was used only to provide a starting ECMP voltage range.

2.2. System design

An electro-chemical–mechanical system (ECMP) was constructed with a vibrating base plate and sample holders that were specifically designed to transfer potential only across the sample surface to the base (Fig. 1). The ECMP consists of a power supply with a feedback system, a power distribution/wire harness assembly, sample holders, a chemical bath, and a vibrating base plate system.

The computer controlled power supply provided the voltage to the connection wires. The application of the voltage was controlled by a feedback system and software controlled operating system that regulated the power based upon the formation of the passivation film on the sample surface. The formation of the film altered the resistance of the system and impacted the measured current. A control system was developed using Labview^{TM} (LabVIEW, 2005) software to allow pulsed voltage regulation and controlled feedback to evaluate the formation of the passivation layer. A data acquisition card (NiPCI 6052E) and a terminal connection (BNC-2110) (both produced by National Labs^{TM}) were used in connection with a standard Microsoft Windows^{TM} based computer to complete the control system.

The voltage was transmitted through the connection wires to a power distribution plate (Ti–6Al–4V, 12 in. × 12 in. × 0.016 in.) and a wire harness which allowed for multiple rotating sample holders to be connected in parallel. Nickel-plated acoustic wire (0.027 in. diameter) was used to connect the power distribution plate and the sample holders. The voltage was transmitted directly to the insulated holders where it was channeled to the back surface of the material sample. The holders were approximately 4.5 in. high, including the main conductive screw, and were constructed of a 316SS alloy holder-weight that rested on a non-conductive polymer base (polyvinyl chloride). The base had an O-ring attached to the outer diameter to allow rotation and insulation against the metallic vibrating base plate.

The sample was held in place within the holder base using Teflon^{TM} screws. The sample was mounted in a conductive mounting compound allowing for electrical conductivity. A conductive threaded screw (main screw) with one hollow end transmitted the applied voltage through the assembly and onto a flat head that the sample is held against. The threaded screw allowed adjustment of the specimen height. The weight was not threaded but was held in place by a 316SS alloy nut that was connected to the main screw.

The holders rotated in an alkaline bath (Allied^{TM} 0.05 colloidal silica solution mixed with an equal amount of distilled water) upon a polishing cloth. The holder's base ensured the current flowed through the specimen face, through the alkaline bath, and into the base plate. The rotational speed of the sample holder was controlled by adjusting the frequency of the base plate. The electrical current across the specimen face was measured using a Fluke^{TM} 8845A precision multimeter. The electrical information was fed-back into the control system to optimize the removal conditions.

Upon applying electrical current through the apparatus, chemical reactions between the surface material and the alkaline bath medium resulted in multiple changes in the immersed sample surface. As oxide layers developed or receded (depending on the applied potential), the alkaline bath chemistry was altered. The sample surface changed and mechanically polished as it rotated against the base plate covered with the suspended silicon electrolyte. By controlling the voltage and bath chemistry, the material

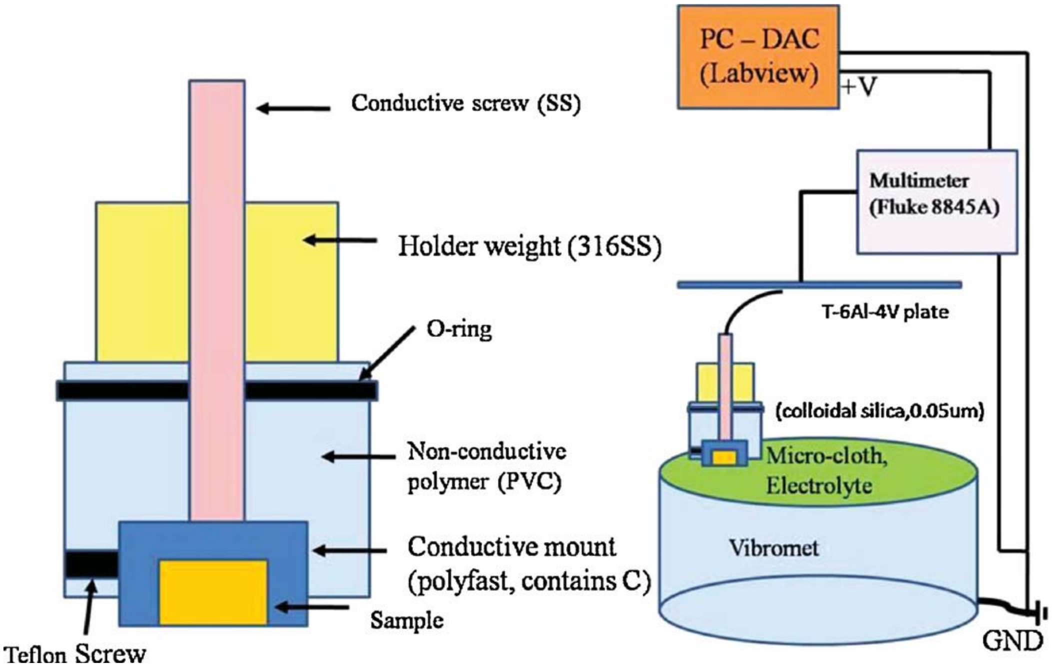

Fig. 1. Schematic of electro-chemical–mechanical polishing system with sample holder.

surface was polished with the chemical reactions augmenting the mechanical polishing and reducing surface damage. The ECMP apparatus was used without applied voltage to compare traditional mechanical polishing, with the same holders and weights.

2.3. Experimental procedures

The anodic behavior of nickel alloys and titanium alloys in the polishing solution was tested using a potential dynamic test system that tracked the potential difference of a 1 in.^{2} coupon immersed in the electrolyte solution (Allied 0.05 colloidal silica solution mixed with an equal part of distilled water). Sheet samples of both Ti–6Al–4V and IN200 were tested using a standard potential dynamic test rig by applying a current across the sample and measuring the potential in reference to a standard hydrogen potential probe. The samples were wiped with a Scotchbrite^{TM} pad and cleaned with isopropyl alcohol prior to the test to remove oxide layers that may have formed. Each alloy system was tested multiple times over a range of electrical densities. The results provided voltage ranges to generate oxide layers within the room temperature electrolyte pH ranges.

Samples of Ti–6Al–4V and IN718 were cut from stock using a diamond saw and mechanically ground and then polished down to a finish stage with a 3-μm suspended diamond slurry using an automatic sample polishing system to reduce variability in preparation procedures. To measure removal rate, indentation marks were applied on the polished surface using a Vickers^{TM} hardness tip loaded at 500 g. The indentation depths were measured from SEM secondary electron images. The samples were polished in the ECMP at different voltages and re-imaged with the SEM to determine the change in the indentation depth. The samples were tested at the optimum voltages under cyclic conditions. Positive voltage was applied for a specific amount of time, and then the negative voltage at the same absolute value was applied for the same time. The alternating voltages applied to the sample helped create and then remove the passivation layers that formed on the sample surface. To assure consistency in testing conditions, the polishing solution and cloth were replaced before every test and the vibration frequency of the base plate for all conditions was maintained for all tests. The depths of the indents were evaluated at 30 min and 250 min intervals for a variety of voltages.

Following the initial testing of removal rates, Ti–6Al–4V and Ni 718 samples were re-tested at the optimum conditions and imaged using a Quanta^{TM} FEI scanning electron microscope operating at 10 kV and a magnification of 300×. For subsurface damage assessments, the samples were also evaluated using an XL30^{TM} FEI scanning electron microscope equipped with a TSL EBSD system operating at 20 kV at a magnification of 350×. The samples were evaluated from large EBSD scans that resulted from stitching small beam/stage controlled scans using a software program written by a Labview^{TM} (LabVIEW, 2005) specifically for this work. The Ti–6Al–4V sample was run for 60 min in the ECMP and evaluated using the EBSD system. The sample was then removed from the SEM and re-prepared starting with 600-grit sandpaper and mechanically polished down to a finish stage with a 3-μm suspended diamond slurry as previously mentioned. The sample was then placed in the ECMP for 250 min and then evaluated using the same EBSD technique and parameters utilizing the indentations to find the previously evaluated region. The procedure was repeated for the IN718 sample, only grid markers placed on the perimeter of the sample were used to locate the same region for EBSD analysis.

X-ray photoelectron spectroscopy (XPS) was performed on the surfaces of the Ti–6Al–4V samples using a Surface Science Instruments^{TM} M-Probe with monochromatic Al Kα X-rays (energy 1486.6 eV). The technique was employed to determine the chemistry of the surface layers and to compare the thicknesses of the formed oxides. Depth profile analyses were acquired by sputtering of the respective sample surfaces with an argon ion gun (1 keV, 10 mA, 6 Torr argon) for 20 s followed by data collection of the Ti 2p (448–470 eV) and O 1s (522–540 eV) regions for 15 s each. This cycle was repeated 20 times for a total sputtering time of 400 s. CasaXPS^{TM} software was used for curve fitting and interpretation of XPS signals.

To further evaluate the quality of the subsurface of the ECMPed sample, transmission electron microscopy (TEM) foils were extracted from a surface normal to the polished surface through focused ion beam (FIB) methods. Prior to milling, the surface of the sample was carbon coated followed by platinum deposition to protect the surface layer from the ion beam milling. The FIBed sample was then analyzed using a Titan 80–300 kV TEM. High resolution electron energy loss spectroscopy (EELS) spectrum profile was obtained across the sample in the STEM mode, with an aberration corrected sub-angstrom probe.

3. Results and discussion

3.1. Removal rates

To optimize the parameters of the ECMP technique, the current density values from the potential dynamic tests were used to provide the starting ranges. Unfortunately, the mounting compound used in the experiment altered the true current density of the surface during the tests. This was compounded by the changing properties of the silica solution and the polishing cloth as the surface of the sample was polished.

Under constant applied voltages, the +0.08 V potential for 30 min provided the highest removal rate for Ti–6Al–4V (3.2 nm/min). The +5 V potential for 30 min provided the highest removal rate for IN718 (7.9 nm/min). The rates were measured by comparing the depth of the Vickers^{TM} indent using optical microscopy. The removal rates reflected the generation of passivation layers followed by removal of the layers by mechanical polishing. Additional tests optimized the conditions by cycling the voltage. Cycling the voltage impeded oxide and hydride formation and accelerated the removal of the passivation layers by mechanical polishing. Figs. 2 and 3 show removal rates obtained by alternating the applied voltage from positive to negative over a specific cycle rate. The results indicate that the ±0.08 V for 210 s provided the highest removal rate for Ti–6Al–4V (6.25 nm/min). The ±5 V for 90 s provided the highest removal rate for the IN718 samples (8.33 nm/min). The data confirmed that applying cyclic potentials provided higher removal rates compared to anodizing or mechanical polishing without an applied potential.

3.2. X-ray photoelectron spectroscopy (XPS) analysis

The anodic layer was evaluated using X-ray photoelectron spectroscopy (XPS). A Ti–6Al–4V sample was polished to a finish stage with a 3-μm suspended diamond slurry. This sample was compared to two Ti–6Al–4V samples that were polished using the ECMP. The first of the two ECMPed samples was polished to a finish stage with 3-μm suspended diamond slurry and placed in the electrolyte with a +0.08 V potential for 1 h. The second of the ECMPed samples was also polished to a 3a finish stage with a 3-μm suspended diamond slurry, but placed in the electrolyte with a −0.08 V potential applied for 1 h. The three samples were analyzed using a multi-sample stage to compare oxide layer formation.

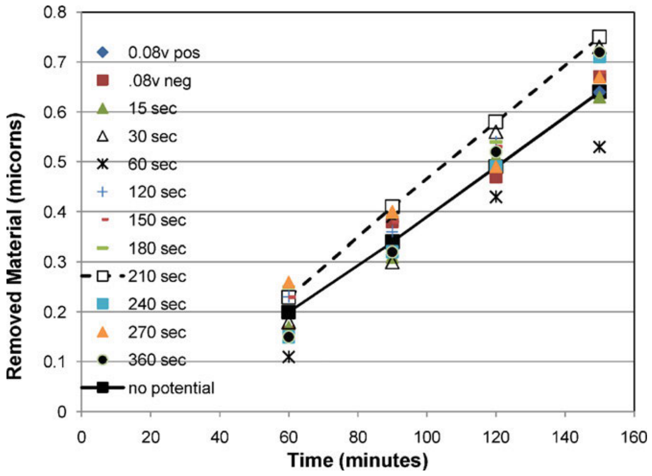

Fig. 2. The effect of time on the thickness of removed titanium at 0.08 V constant and oscillating applied potential.

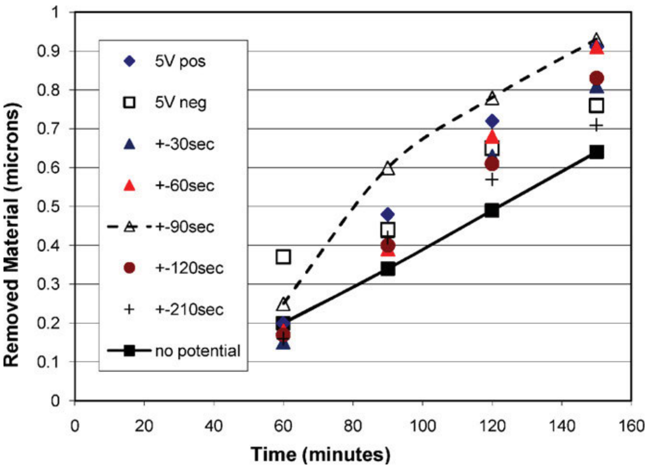

Fig. 3. The effect of time on the thickness of removed nickel removal at 5 V constant and oscillating applied potential.

Observation of the Ti 2p region for the base and ECMP samples indicated the presence of an oxidized titanium layer at each of the sample surfaces. Depth profile analysis through the oxidized layer into the underlaying metal suggested that the oxidized layer was thicker in both of the ECMP samples. This trend can be visualized through observation of the Ti 2p$^{3/2}$ peak in the spectral data found in Fig. 4. The Ti 2p$^{3/2}$ peak is initially observed at 458.4 eV indicating that titanium is present in its oxidized state. After controlled sputtering of the sample surface the Ti 2p$^{3/2}$ peak gradually shifted to 453.7 eV representative of metallic titanium. In the base Ti–6Al–4V sample this transition takes *ca.* 60–80 s of total sputtering time to completely move through the surface oxide layer. Sputtering times of *ca.* 180–200 and *ca.* 200–220 s were required to move through the oxide layer in the negative and positive ECMPed samples, respectively. Under the described operating conditions a sputtering rate of *ca.* 0.1 nm is observed for a 10 nm SiO_2 standard, which suggested an approximate thickness of the oxide layer for the base sample to be 6–8 nm compared to an approximate thickness of 18–22 nm for the ECMP processed samples. Similar trends were observed for the O 1s spectral region (Fig. 5) which demonstrated a significant loss of oxygen at the sample surface as sputtering time was increased. The results agreed with the potential dynamic data reported elsewhere (Korb, 1994).

3.3. Electron energy loss spectroscopy (EELS) spectrum profile analysis

The STEM image in Fig. 6 shows the region near the surface where the EELS line profile analysis was performed. The dark region near the surface of the sample was an artifact introduced possibly during the FIB process. The EELS spectra were obtained in the energy range 450–600 eV in order to observe the changes in Ti-L absorption edge. EELS spectra were continuously recorded at 1 nm intervals from the surface of the sample to the interior. Typical examples of the EELS spectra taken from the locations 1–3 on the sample were illustrated in Fig. 6. The spectra taken from the locations 1 and 2 showed the Ti-L peak position at ∼465 eV. On the other hand, the same Ti-L peak can now be seen at ∼470 eV in the spectrum obtained near the surface at location 3. This shift of about 5 eV in the Ti-L peak position has been recorded up to a depth of 6–8 nm from the surface of the sample. This peak shift is indicative

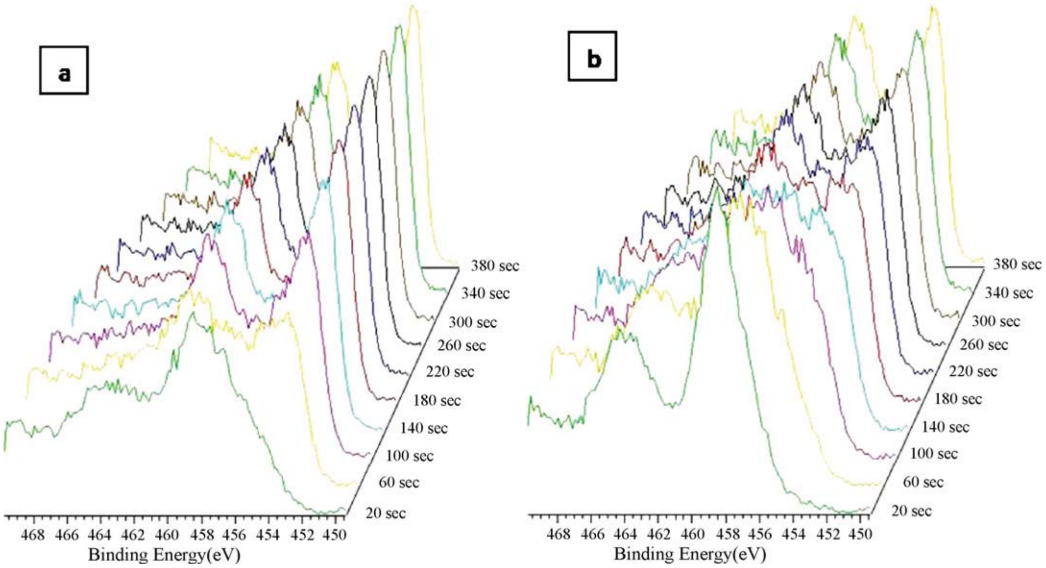

Fig. 4. XPS binding energy (eV) versus sputtering time (s) results for the Ti 2p peaks for the titanium samples: (a) unprocessed and (b) processed with negative potential. Sputtering conditions were identical.

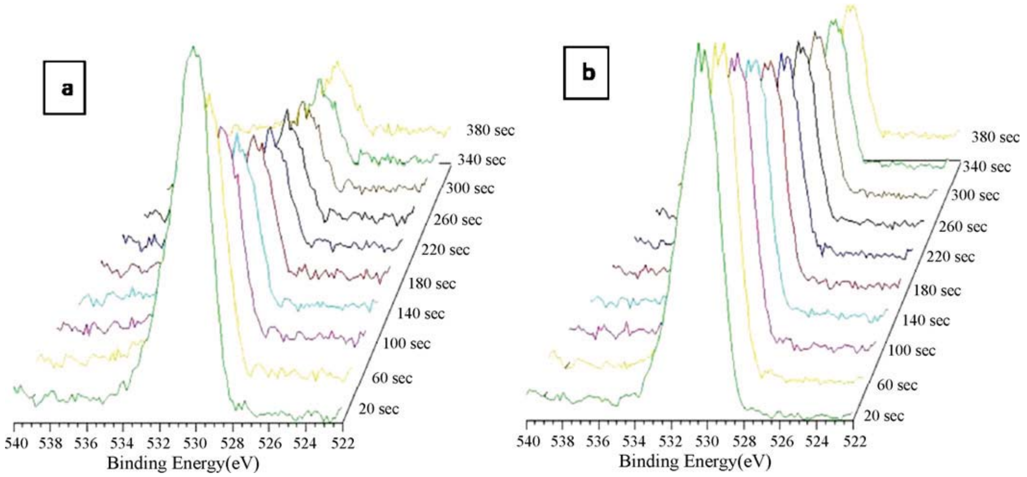

Fig. 5. XPS binding energy (eV) versus sputtering time (s) results for the O 1s peaks for the titanium samples: (a) unprocessed and (b) processed with negative potential. Sputtering conditions were identical.

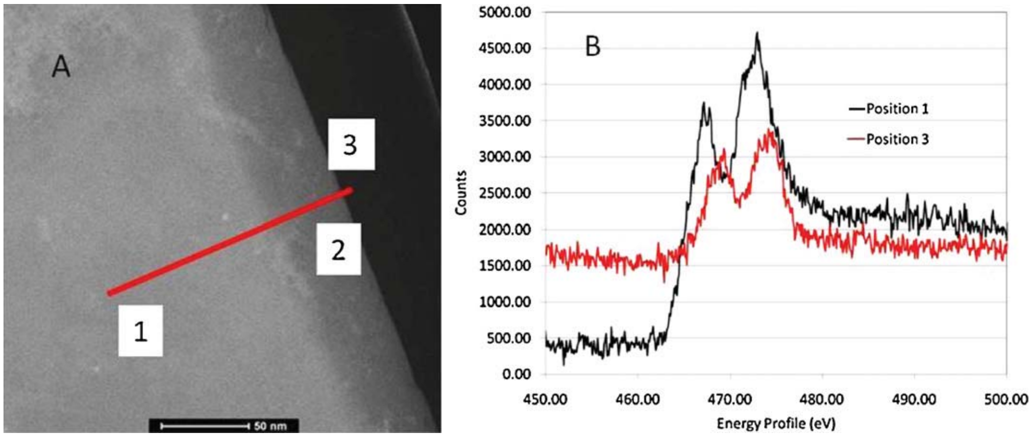

Fig. 6. (a) STEM-HAADF image showing the region beneath the polished surface with positions 1, 2, and 3 and (b) EELS spectrums obtained from the marked postions 1 and 3 in the sample show the relative shift in the Ti-L peak positions. Position 2 did not show any shift from position 1.

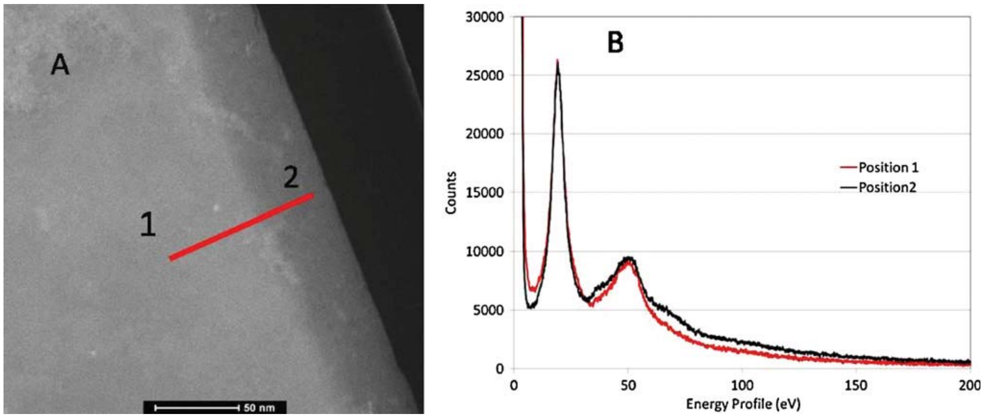

Fig. 7. (a) STEM-HAADF image showing the region beneath the polished surface with positions 1 and 2. (b) EELS spectrums obtained from the marked postions 1 and 2 in the sample show the plasmon peak postions. There was no shift in peak positions.

of O_2 near the surface. This is consistent with the results obtained from the XPS experiments mentioned above.

The dark region near the surface of the sample was closely examined for any hydride formation during the electrolytic process. Once again EELS line profile analysis was performed, now in the low-loss region (0–100 eV), to observe any changes in the plasmon peaks. The results are shown in Fig. 7 for positions 1 and 2. An earlier study (Kihn et al., 2005) had reported that the titanium hydride formation can introduce a peak shift in the range of 5–8 eV in the plasmon peak position. No such shifts were seen in the spectra obtained. Hence, it is suggested that the dark region is indeed an artifact in the sample.

3.4. Subsurface damage

Subsurface damage was assessed using the image quality (IQ) values from TSL^{TM} EBSD scans. For titanium and nickel alloys, analysis of the samples after ECMP for 60 min compared favorably to the samples processed without applied potential after 250 min. For the Ti–6Al–4V samples, the samples processed without applied potential provided an average IQ of 4117, compared to the value of 3920 for the sample ECMPed using the ±0.8 V for 210 s cycle. For the NI 718 samples, the sample ECMPed with ±5 V, 90 s cycle conditions provided an average IQ value of 6875, compared to the value of 5255 obtained using no potential. Processing of the Ti–6Al–4V and IN718 samples with the ECMP for longer times further improved the IQ values.

4. Conclusions

The electrochemical–mechanical polishing system (ECMP) removed material from titanium and nickel alloys at a higher rate than the chemical–mechanical system. The removal rates for examined alloys were increased under alternating direct voltage conditions at different intervals. The electrochemical reaction produced a surface film that was then removed by the mechanical agitation of the polishing medium.

Applying a current in connection with the alkaline electrolyte produced an oxide layer on the surface of Ti–6Al–4V samples with a thickness approximately twice the thickness forming on the sample that was processed without applying current.

The EBSD results indicated lower surface and subsurface damage achieved using the ECMP for the titanium and nickel alloys. The distribution of image quality (IQ) values indicated similar results after 1 h ECMP compared to 2.5 h of only chemical–mechanical polishing (i.e. no current).

EELS and XPS analysis showed a shift in the energy absorption edges of Ti–6Al–4V samples indicating the formation of titanium oxide at the surface of the ECMP sample. No evidence of hydride formation was found upon further analysis of the interface.

Acknowledgements

This research work was conducted as part of the in-house research activities of the Hot Metallic Structures program at the Air Force Research Laboratory's Materials and Manufacturing Directorate. The authors are grateful to Dr. Natasha Voevodin for the corrosion analysis and potential dynamic testing. Mr. Kevin Shiveley II was supported by Air Force Contract FA8650-08-D-5200, Dr. Gopal Viswanathan was supported by Air Force Contract FA8650-10-D-5226, and Mr. Adam Shiveley was supported by Air Force Contract FA8650-07-D-5800.

References

Bieler, T., Goetz, R.L., Semiatin, S.L., 2005. Antisotropic plasticity and cavity growth during upset forging of Ti–6Al–4V. Materials Science and Engineering A 405, 201–213.
Boinet, M., Maximovitch, S., Dalard, F., DeBouvier, O., 2003. Study of nickel passivation in a borate medium. Journal of Materials Science 38, 4041–4046.
Bonifas, A.M., Taylor, E.J., Sun, J.J., 2004. Industrial applications of advanced electrochemical finishing techniques. American Society of Mechanical Engineers 15, 199–205.
Collins, P.C., Welk, B., Searles, T., Tiley, J., Russ, J.C., Fraser, H.L., 2009. Development of methods for the quantification of microstructural features in alpha plus beta-processed alpha/beta titanium alloys. Material Science and Engineering A 508, 174–182.
Du, H.L., Datta, P.K., Leiws, D.B., Burnell-Gray, J.S., 1996. High-temperature corrosion of Ti and Ti–6Al–4V alloy. Oxidation of Metals 45, 507–527.
Fontana, M.G., 1986. Corrosion Engineering. McGraw Hill.
Jones, D.A., 1996. Principles and Prevention of Corrosion. Prentice Hall.
Kihn, Y., Mirguet, C., Calmels, L., 2005. EELS studies of Ti-bearing materials and ab initio calculations. Journal of Electron Spectroscopy and Related Phenomena 143, 117–127.
Kissinger, R.D., 1996. Superalloys 1996. Minerals, Metals, and Materials Society, Warrendale, PA.
Korb, L.J., 1994. ASM Handbook: Volume 13: Corrosion. ASM International, Metals Park.
Lee, J.M., McCrabb, H., Taylor, E.J., Carpio, R., 2006. Current distribution for the metallization of resistive wafer substrates under controlled geometric variations. Journal of Electrochemical Society 153, C265–271.
Luetering, G., et al., 2003. Titanium. Springer-Verlag.
$\text{LabVIEW}^{\text{TM}}$ [Computer Software], 2005. National Instruments.
Meisenkothen, F., Wheeler, R., Uchic, M.D., Kerns, R.D., Scheltens, F.J., 2009. Electron channeling: a problem for X-ray microanalysis in materials science. Microscopy and Microanalysis 15, 83–92.
Montemor, M.F., Ferreira, M.G.S., Hakki, N.E., Da Cunha Belo, M., 2000. Chemical composition and electronic structure of the oxide films formed on 316L stainless steel and nickel based alloys in high temperature aqueous environments. Corrosion Science 42, 1635–1650.
$\text{National Instruments}^{\text{TM}}$ [Computer Hardware], 2008. National Instruments.

Reed, R.C., 2006. The Superalloys. Cambridge University Press, New York.

Reidenbach, F., 1994. ASM Handbook: Volume 5: Surface Engineering. ASM International, Metals Park.

Salem, A.A., Semiatin, S.L., 2009. Antisotrophy of the hot plastic deformation of Ti–6Al–4V single-colony samples. Materials Science and Engineering A 508, 114–120.

Sniegowski, J.J., 1996. Chemical–mechanical polishing: enhancing the manufacturability of MEMS. Proceedings of SPIE—The International Society for Optical Engineering 2879, 104–115.

Steigerwald, Murarka, S.P., Gutmann, R.J., Duquette, D.J., 1995. Chemical processes in the chemical mechanical polishing of copper. Materials Chemistry and Physics 41, 217–228.

TexSEM Laboratories, 2001. OIM DC Users Manual. TexSEM Laboratories, USA.

Tiley, J., Searles, T., Lee, E., Kar, S., Banerjee, R., Russ, J.C., Fraser, H.L., 2004. Quantification of microstructural features in α/β titanium alloys. Materials Science and Engineering A 372, 191–198.

Tiley, J., Viswanathan, G.B., Srinivasan, R., Banerjee, R., Dimiduk, D.M., Fraser, H.L., 2009. Coarsening kinetics of γ' precipitates in the commercial nickel base Superalloy Renè 88 DT. Acta Materialia 57, 2538–2549.

Tiley, J., Viswanathan, G.B., Shiveley, A., Tschopp, M., Srinivasan, R., Banerjee, R., Fraser, H.L., 2010. Measurement of γ' precipitates in a nickel-based superalloy using energy-filtered transmission electron microscopy coupled with automated segmenting techniques. Micron 41, 641–647.

TSL$^{\text{TM}}$ OIM Analysis [Computer Software], 2008. TexSEM Laboratories.

Vander Voort, G.F., 2004. Metallography Principles and Practice. ASM International, Metals Park.